XMM-Newton CCF Release Note

XMM-CCF-REL-176

RGS QUANTUMEF Shortest-Wavelength Correction Factors

A.M.T. Pollock

July 27, 2004

1 CCF components

Name of CCF	VALDATE	List of Blocks changed	XSCS flag
RGS1_QUANTUMEF_0013	1998-01-01T00:00:00	RGA_EFFAREACORR SI1 SI2 SI3 SI4 SI7	NO
RGS2_QUANTUMEF_0014	1998-01-01T00:00:00	RGA_EFFAREACORR SI1 SI2 SI3 SI4 SI5 SI7	NO

2 Changes

Near the short-wavelength end of the RGS bandpass, the instrument model breaks down and the detected count rate falls off more quickly with decreasing wavelength than expected from the scalar diffraction theory that forms the basis of the calibration. This is illustrated in Fig.1 which shows a variety of fluxed spectra from Mkn421. The flux decrease at the shortest wavelengths is clear. What is less clear is where the trouble starts. Fig.2 shows details of the empirical approach adopted to model the deficit. By inspection, the spectrum falls into three parts: between $7 \leq \lambda(\text{Å}) \leq 10$ the spectrum is OK and serves as the basis for extrapolation to shorter wavelengths; down to $\lambda \approx 5.7$Å the spectrum falls quite steeply; while at even shorter wavelengths, where no claims are made for the reliability of the instrument model, the observed flux first flattens before becoming

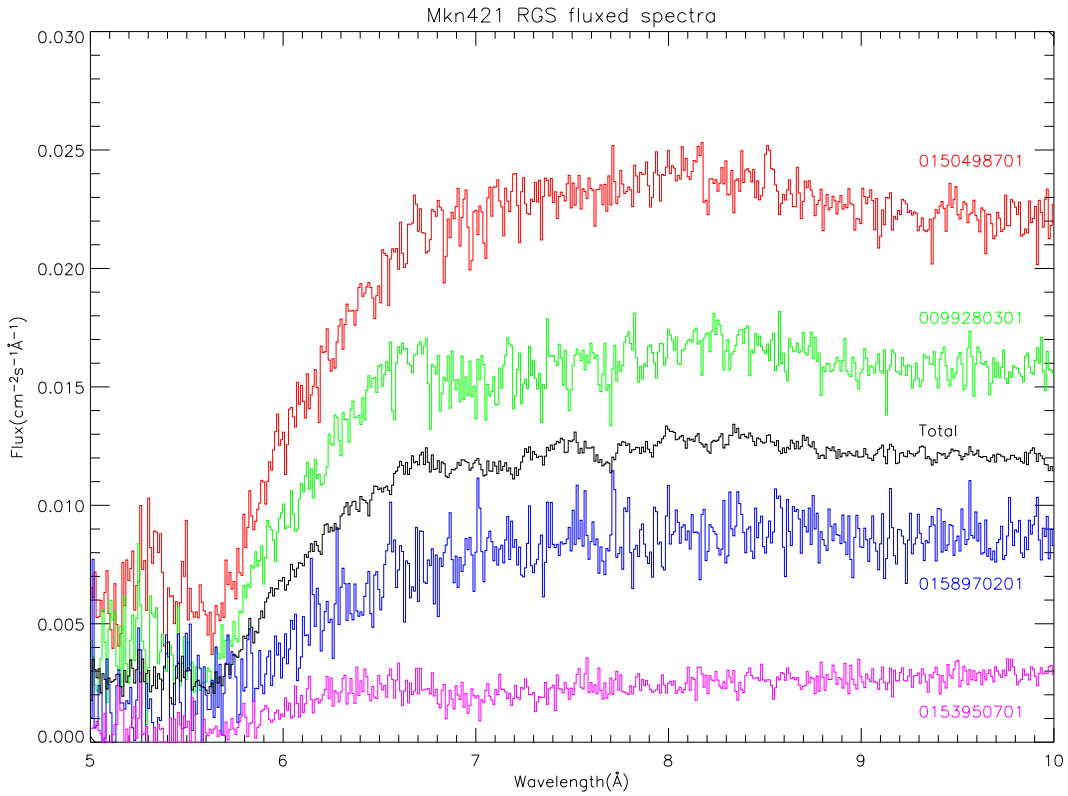

Figure 1: Mkn421 has been observed many times for calibration purposes with XMM. It is variable both within and between observations. Shown here are averaged fluxed spectra below 10Å calculated by the SAS task `rgsfluxer` that combine the first and second orders of RGS1 and RGS2. The brightest, faintest and two intermediate observations are shown along with a total spectrum resulting from 88 spectra in 22 observations.

entirely dominated by noise. The data below about 6Å are shown for completeness and are not recommended for use.

Assuming no differences between RGS1 and RGS2 and orders 1 and 2, the reliable spectrum between $7 \leq \lambda(\text{Å}) \leq 10$ was modelled using the `IDL svdfit` routine with a combination of Legendre polynomials that was extrapolated to shorter wavelengths to provide the reference flux for the deficit determination. The extrapolation follows the data a little further down to 6.7Å, close to the Silicon edge, where the deficit seems to start. The observed deficit was smoothed in turn with two further sets of Legendre polynomials as shown by the green and blue stretches of data in Fig. 2.

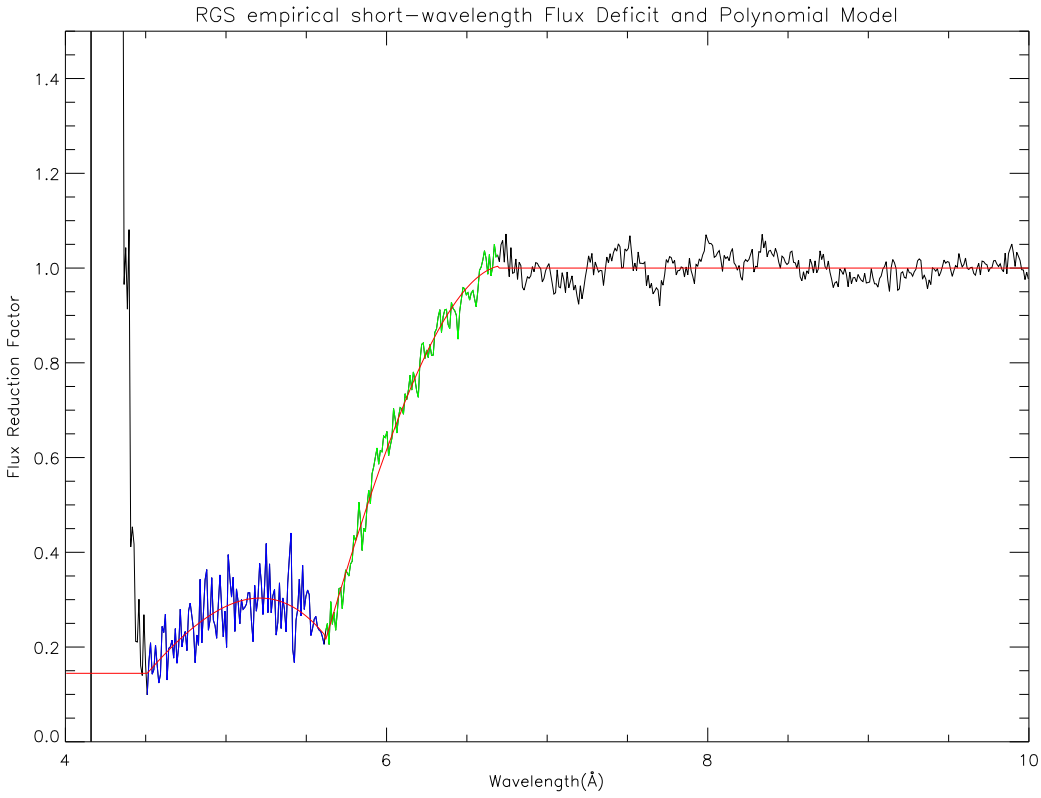

Figure 2: The empirical flux reduction factor in red calculated from the mean fluxed spectrum of Mkn421. The green and blue stretches of data delineate wavelength ranges in which the deficit apparently behaves differently as modelled by separate sets of polynomial coefficients.

The changes described above concern the first use of the RGA_EFFAREACORR extensions for supplying empirical short-wavelength correction factors to the effective area model. At the same time the opportunity has been taken to bring up-to-date data concerning the thicknesses of some CCDs held for completeness in the MTHICK header keywords of the extensions [SI1,...,SI9]. These data are not used currently in the calibration model. The CCD PI redistribution model relies instead on a method parameterized according to independent data held in the RGS%_REDIST CCFs.

3 Scientific Impact of this Update

The wavelength range between 6 and 7Å contains important lines of SiXIII and SiXIV which, especially in the case of the He-like triplet at $\lambda\lambda$6.648,6.688,6.740, are often strongly detected in RGS spectra.

4 Estimated Scientific Quality

This CCF update should allow users to assign SiXIII or SiXIV line fluxes that are reliable to 10 or 20% or to model spectra down to 6Å with a similar level of reliability.

5 Test procedures & results

Although the CCF update is expected to be useful for the analysis of He-like and H-like lines of Silicon, the quality of the correction is best assessed through analysis of smooth continuum blazar spectra which are likely, over the restricted wavelength range of interest here, to be well described by power-laws. Fig. 3 shows the XSPEC power-law models derived using response matrices based on the new RGS QUANTUMEF CCFs for one observation of PKS2155-304 and three of Mkn421. With the new corrections, the power-law models work quite well even below 6Å.

6 Expected Updates

None.

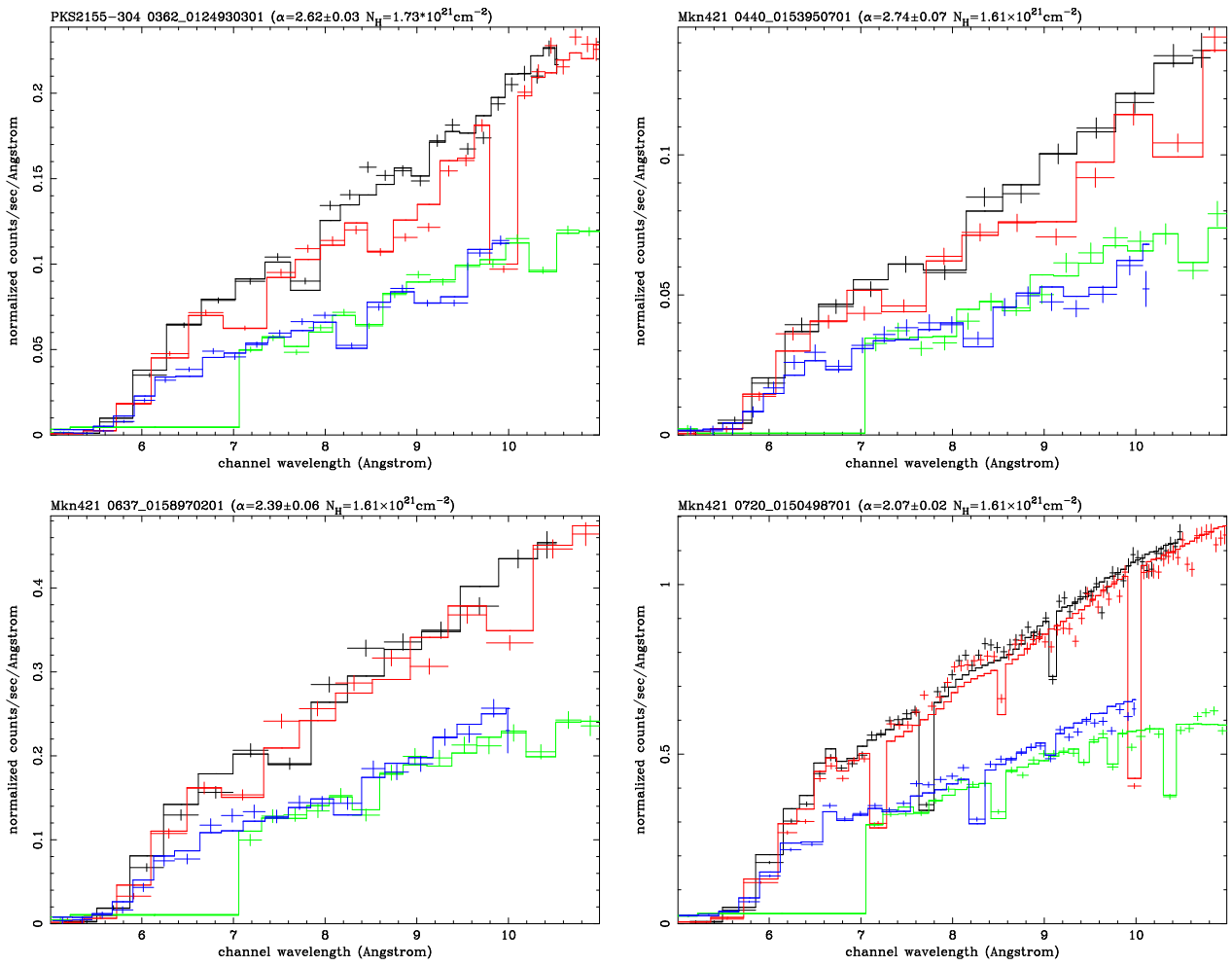

Figure 3: Some example XSPEC analysis of blazar spectra using response matrices calculated with the new short-wavelength correction CCFs. Short wavelength parts of RGS1 and RGS2 1st (black and red) and 2nd order (green and blue) spectra are compared with power-law models of one observation of PKS2155-304 and three of Mkn421, which flattens as it brightens. The three Mkn421 spectra are the brightest, the faintest and an intermediate case. The best-fit power-law indices, α, are shown. The absorbing column densities were fixed at their galactic values as indicated, although these are of little relevance at such high energies.